Quantitative determination of the absorption spectra of chromophores in strongly scattering media: a light-emitting-diode based technique

Sergio Fantini, Maria Angela Franceschini, Joshua B. Fishkin, Beniamino Barbieri, and Enrico Gratton

The absorption and scattering coefficient of a macroscopically homogeneous strongly scattering medium (lipid emulsion) containing Methylene Blue is quantitatively measured in the spectral range from 620 to 700 nm. We conduct the measurements in the frequency domain by using a light-emitting diode (LED) whose intensity is modulated at a frequency of 60 MHz. We derive an analytical expression for the absorption and scattering coefficients that is based on a two-distance measurement technique. A comparison with other measurement protocols such as measurement at two modulation frequencies shows that the two-distance method gives a better determination of the scattering and absorption coefficients. This study highlights the efficiency and ease of use of the LED technique, which lends itself to *in vivo* spectroscopy of biological tissues.

Key Words: Frequency domain, absorption and scattering coefficients, diffusion approximation, strongly scattering medium, biological tissue, photon migration.

1. Introduction

The quantitative determination of the absorption spectrum of a substance dissolved in a highly scattering medium is not a trivial problem and is of particular interest in a number of medical applications. For example, a quantitative measurement of the absorption coefficient in tissues can detect the presence and concentration of certain exogenous or endogenous chromophores. The former may be drugs whose distribution and metabolism in tissues can then be dynamically monitored; examples include chemical markers for tumors such as Indocyanine Green and hematoporphyrin derivative,[1] or photosensitizing agents for photodynamic therapy.[2] In the near-infrared region the endogenous chromophores are typically heme proteins such as hemoglobin, whose absorption characteristics depend on the oxygenation state that is affected by metabolic processes,[3] cytochrome aa_3 in both reduced and oxidized form, melanin, and bilirubin. Furthermore, knowledge of the optical properties of tissues can provide real-time information on the fluence distribution of light during therapeutic procedures such as photodynamic therapy[4] or laser surgery.[5]

In a steady-state transmission experiment, the absorption coefficient (μ_a) is related to the incident (I_0) and transmitted (I) light intensity by the Beer–Lambert law:

$$\mu_a = \frac{1}{L}\ln\left(\frac{I_0}{I}\right) = \epsilon[c], \tag{1}$$

where L is the photon path length (centimeters), ϵ is the extinction coefficient (inverse centimeters times inverse micromolars) and $[c]$ is the concentration of the absorber (micromolars). In the absence of scattering processes, path length L corresponds to the thickness of the sample, and from a measurement of I and I_0 one directly determines μ_a. By contrast, the presence of scattering particles in the medium gives rise to a distribution in path length whose mean value $\langle L\rangle$ can be substantially greater than the geometrical thickness of the sample. Furthermore, the two physi-

When this research was performed, B. Barbieri was with ISS, Inc., 2604 North Mattis Avenue, Champaign, Illinois 61821, and S. Fantini and M. A. Franceschini were with the Istituto di Elettronica Quantistica, Consiglio Nazionale delle Ricerche, Via Panciatichi 56/30, 50127 Firenze, Italy. The other authors were with the Laboratory for Fluorescence Dynamics, Department of Physics, University of Illinois at Urbana–Champaign, 1110 West Green Street, Urbana, Illinois 61801-3080.

Received 6 July 1993; revised manuscript received 3 January 1994.

0003-6935/94/225204-10$06.00/0.

cal processes experienced by photons in a scattering medium, i.e., absorption and elastic scattering, cause attenuation in the transmitted light intensity as a result of both the annihilation of photons (absorption) and the deflection of photons out of the solid angle of detection (scattering), so Eq. (1) is no longer valid. These two physical processes are described in terms of the linear coefficients μ_a and μ_s, both in units of inverse centimeters, which are, respectively, the inverse of the mean-free path for absorption and scattering. We then observe that Eq. (1) holds only when $\mu_s \ll \mu_a$. In this paper we always refer to the transport scattering coefficient, $\mu_s' = \mu_s(1 - g)$, where g is the anisotropy factor defined as the average of the cosine of the scattering angle. For soft tissues in the near-infrared spectral region, the value of anisotropy factor g is typically in the range 0.7–0.95 (Ref. 6), which means that the scattering is mainly forward directed.

Average photon path length $\langle L \rangle$ depends on both μ_a and μ_s'; it decreases as μ_a increases, and it increases as μ_s' increases. A complication arises in biological tissues in the spectral region where light penetration is adequate, because μ_s' is typically much larger than μ_a and relationship (1) breaks down. The problem of one separating the effects of absorption and scattering, thus measuring μ_a and μ_s' independently, has been treated in two frameworks: steady-state and time-resolved spectroscopy. In steady-state spectroscopy, several methods have been developed. These include the measurement of the ratio of the reflectance at two wavelengths,[7] an integrating sphere method,[8–10] a diffusion model for optically homogeneous and semi-infinite media,[11] the detection of coherent backscatter,[12] and an image-refocusing technique.[13] A general limitation of these techniques is their nontrivial application to *in vivo* diagnostics. The specific complications in the various cases are related to sensitivity to boundary conditions, the necessity of acquiring a large data set, insensitivity to small changes in the optical coefficient, and incompatibility with fiber-optic instrumentation. In contrast, time-resolved spectroscopy, which can be accomplished in the time or frequency domain, is a more promising method for medical applications. In time-domain measurements the optical response of the system to a narrow incident light pulse (<50 ps) provides the time-of-flight distribution, which is related to the average photon path length. By fitting the measured pulse shape to a theoretical expression, one obtains μ_a and μ_s' in turbid media.[14] In frequency-domain measurements the intensity of the light source is modulated at high frequency (10^7–10^9 Hz), and the signal is detected by a phase-sensitive detector. The measured quantities are the phase shift of the detected light relative to the exciting signal (Φ), the average intensity (dc component), and the amplitude of the intensity oscillation (ac component). The measurement of these quantities permits one to determine the absorption and scattering coefficients of the medium (see Subsection 2.D). Frequency-domain measurements provide certain advantages over the time-domain measurements[15]; the chief advantages are the faster data-acquisition times, which permit a study of dynamic processes, and the relatively inexpensive equipment.

This paper describes a general procedure for the quantitative measurement of the absorption spectrum of a substance dissolved in a macroscopically homogeneous strongly scattering medium. The procedure operates in the frequency domain with a modulated light-emitting diode (LED) light source. The choice of a LED as the light source, instead of other typical sources such as lasers or arc lamps, results from several considerations.

(i) Spectral distribution: The wide spectral width of LED's (~40 nm FWHM) allows one to investigate a continuous spectral range of ~80 nm. Currently available LED's emit at different wavelengths that are sufficient to cover the spectral range from 550 to 900 nm, which is the region of interest in medical applications (Fig. 1 shows the spectral distribution obtained from a variety of LED's).

(ii) Ease of modulation: A LED is easily intensity modulated by being driven with a radio-frequency oscillating signal. The efficiency of modulation is limited by the electrical response time of the LED.

(iii) Stable output: The intensity emitted by a LED is stable with respect to that of lasers and arc lamps.

(iv) Safety: The low optical power emitted, typically no more than a few milliwatts, and the wide angular distribution make LED's safe for *in vivo* studies.

(v) Cost effectiveness: The low cost and the relatively simple instrumentation required in the LED technique render it an attractive technology for spectroscopy.

In Subsection 2.B we discuss the characteristic of the LED's that make them suitable devices for applications in frequency-domain spectroscopy.

In addition to the quantitative aspects of spectral acquisition in a scattering medium by the relatively straightforward LED technique, we have developed a simple experimental protocol that allows one to collect data amenable to an analytical solution for μ_a and μ_s'. We derived the algorithm from a previous theoretical development[16] that provided an analytical solution to the Boltzmann transport equation in the diffusion approximation.

2. Experimental Methods

The experimental arrangement is shown in Fig. 2. In this section we discuss the various components of the system, with emphasis on the description of the LED used as the light source. We describe the measurement method and discuss how the solution to the transport equation dictates the choice we made.

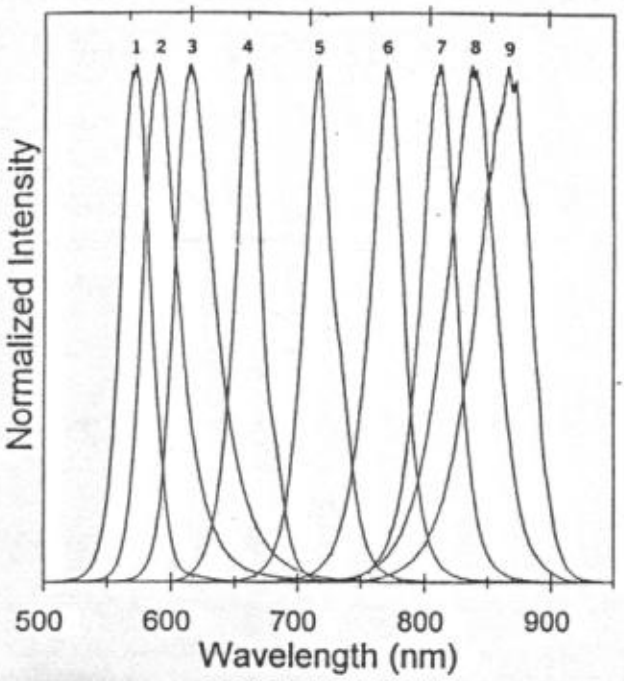

Fig. 1. Spectral emission of nine LED's whose peak wavelengths range from 570 to 870 nm. The superposition of these spectra yields a white-light source in the optical window from 550 to 900 nm. Normalizing the spectra obscures the fact that long-wavelength LED's typically have higher power. The spectra of the LED's were measured with an optical multichannel analyzer (Princeton Instruments, ST-120), while the LED's were modulated at 20 MHz (curves 1–3) and 60 MHz (curves 4–9); the green, yellow, and orange LED's (LED's 1, 2, and 3, respectively) could not be efficiently modulated at frequencies higher than 20 MHz. The numbered spectra refer to the following devices (we list manufacturer, part number, and approximate integrated power emission under the given modulating condition): 1, Hewlett-Packard (H-P) HLMP-3502, 0.002 mW; 2, H-P HLMP-3400, 0.006 mW; 3, H-P HLMP-D401, 0.009 mW; 4, H-P HLMP-4101, 0.2 mW; 5, H-P HEMT-6000, 0.3 mW; 6, Asea Brown Bover; HAFO 1A330, 0.5 mW; 7, H-P HFBR-1402, 0.7 mW; 8, Motorola MFOE1203, 1.5 mW; 9, Asea Brown Bover; HAFO 1A277A, 1 mW.

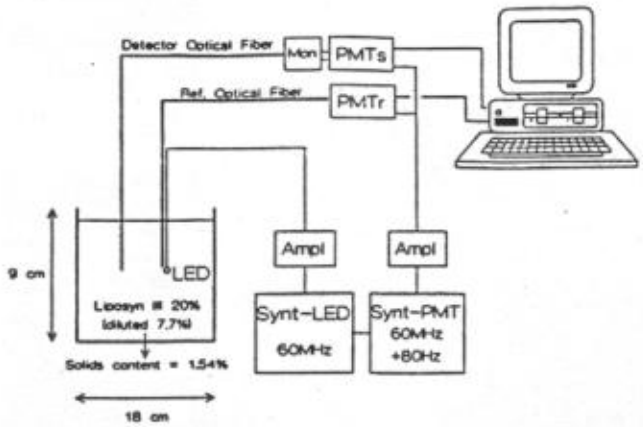

Fig. 2. Experimental arrangement showing the LED immersed in the scattering medium, the source–detector fiber geometry, and the other instrumentation. We used two frequency-locked synthesizers (Synt's) and two amplifiers (Ampl's) to modulate both the LED and the gain function of the photomultiplier tubes (PMT's). PMT*r*, source light collected by reference optical fiber, provides a reference signal against which the phase lag of the measured light, collected by PMT*s* by the detector optical fiber and through the monochromator (Mon), is calculated. The reference channel also compensates for variations in LED intensity by a ratioing method.

A. Absorbing Material and Scattering Medium

As a test absorbing material we selected Methylene Blue (MB). It has a molar extinction coefficient, defined by Eq. (1), of $0.182 \pm 0.001\ \text{cm}^{-1}\ \mu\text{M}^{-1}$ (Ref. 17) at 664 nm, and the maximum absorbance wavelength is 656 nm. Using a standard spectrophotometer (Perkin-Elmer Lambda 5), we measured its absorption spectrum in water between 620 and 700 nm. This spectrum is the control for quantitative comparison with the MB absorption spectra measured in the strongly scattering solution. We have studied different concentrations of MB in the highly scattering medium to obtain the values typical of μ_a in biological tissues, i.e., 10^{-1}–$10^{-2}\ \text{cm}^{-1}$ (Ref. 6).

The scattering medium is an aqueous solution of Liposyn III 20% (intravenous fat emulsion) from Abbott Laboratories. The Liposyn concentration is 7.7% by volume, matching the medium scattering coefficient of $20\ \text{cm}^{-1}$ that is typical for soft tissues.[6] The solids content of the Liposyn emulsion is 1.54% (i.e., 7.7% of 20%). All the measurements are conducted in a 2.3-L cylindrical container whose dimensions, as shown in Fig. 2, are 9 cm × 18 cm.

B. Light Source

Figure 1 provides a spectral chart for the selection of an appropriate LED source for a particular application. The absorption spectra of MB overlaps with LED 4. This LED is a double-heterojunction AlGaAs–GaAs red LED manufactured by Hewlett-Packard (HLMP-4101). Among all the red LED's we tested, this device was the most efficiently modulated. We found that the GaAsP red LED's were not suitable devices for our purposes: even those with a fast response (10 ns) were not sufficiently intense when modulated at tens of megahertz. In contrast, almost all the LED's in the infrared region (Fig. 1, LED's 5–9) showed both fast response times and good intensity characteristics, with efficient modulation up to 100–150 MHz. Modulation of the LED's intensity is accomplished by the application of a sinusoidal voltage. We use a Marconi Instruments 2022A signal generator output amplified by an Electronic Navigation Industries 403LA rf amplifier. No dc offset is added to the sinusoidal exciting signal sent to the LED so that the LED has enough time to turn off during the negative front. We did not utilize a clamping diode to cut the negative front of the sinusoidal voltage, because the reverse breakdown voltage of the LED we used (15 V) is greater than the maximum peak voltage we employed. We studied the dc and ac light-intensity behavior at different modulation frequencies and peak excitation voltages. We did this to find the best compromise between the requirements of

high modulation frequency (a frequency-domain measurement is more accurate at higher modulation frequencies) and high ac signal (which improves the signal-to-noise ratio). We found that the best working point for our LED is a 60-MHz modulation frequency with a 5-V peak excitation. In these working conditions, the modulation ratio (ac to dc light-intensity component) is 60% in air, the total emitted light power is ~0.2 mW, the peak wavelength is 665 nm, and the spectral line full width is 30 nm. The tails of the spectral distribution allow us to accomplish measurements in the broader range of 620 to 700 nm, which is an appropriate wavelength region for the measurement of the absorption spectrum of MB (λ_{max} = 656 nm).

C. Fiber-Optics and Detectors

The detector fiber optics consists of a bundle of glass optical fibers with an overall diameter of 3 mm, whose output was dispersed with a monochromator (10-cm ISA Instruments SA) and detected by a Hamamatsu R928 photomultiplier tube (PMTs). A second photomultiplier tube (PMT*r*) collects a reference signal from a 1-mm-diameter plastic optical fiber in close contact with the LED (Fig. 2). We used this PMT*r* signal both as a reference for the phase measurements and for compensating variations in LED intensity that might occur during the measurement (less than 5%). A cross-correlation electronics system processed the photomultiplier signals by using a digital acquisition method.[18] In our measurement the cross-correlation frequency was set to 80 Hz. The geometrical configuration of the detector optical fiber with respect to the LED source (see Fig. 2) was such that only scattered (not ballistic) photons were detected, and the walls of the container, as well as the surface of the liquid solution, were far enough from the LED and the detector fiber tip to ensure the validity of an infinite medium approximation.

D. Measurement Technique

To discuss our measurement technique, we recall the starting equations from which μ_a and μ_s' can be determined.[16] The theoretical background is the diffusion approximation to the Boltzmann transport equation, which is valid as long as $\mu_a \ll \mu_s'$ and points far from sources and boundaries (where far means at distances much greater than the photon mean-free path). An analytical solution has been obtained in the frequency domain for a homogeneous infinite medium under the assumption that the modulation frequency ($\omega/2\pi$) is much smaller than the typical frequency of the scattering processes (i.e., $\nu\mu_s'$ where ν is the speed of light in the medium). Fishkin and Gratton obtained the following expressions for the experimentally measured quantities from this solution, and they are valid at source–detector separations r much greater than the photon mean-free path[16]:

$$\Phi = r\left(\frac{\nu^2\mu_a^2 + \omega^2}{\nu^2 D^2}\right)^{1/4} \sin\left[\frac{1}{2}\arctan\left(\frac{\omega}{\nu\mu_a}\right)\right], \quad (2)$$

$$\ln(rU_{dc}) = -r\sqrt{\frac{\mu_a}{D}} + \ln\left(\frac{S}{4\pi\nu D}\right), \quad (3)$$

$$\ln(rU_{ac}) = -r\left(\frac{\nu^2\mu_a^2 + \omega^2}{\nu^2 D^2}\right)^{1/4} \cos\left[\frac{1}{2}\arctan\left(\frac{\omega}{\nu\mu_a}\right)\right] + \ln\left(\frac{SA}{4\pi\nu D}\right), \quad (4)$$

where Φ is the phase shift of the detected signal relative to the exciting signal, U_{dc} is the dc component of the photon density, U_{ac} is the amplitude of the ac component of the photon density, r is the distance between source and detector, ν is the speed of light in the medium (given by c/n with n index of refraction of the medium), ω is 2π times the modulation frequency, D is the diffusion coefficient defined as $1/(3\mu_a + 3\mu_s')$, S is the source strength (in photons per second), and A is the modulation of the source (the modulation of an intensity-modulated light source is defined as the ratio of the ac to the dc component of the intensity). The conditions under which these equations are valid ($\mu_a \ll \mu_s'$, $\omega/2\pi \ll \nu\mu_s'$) are well satisfied by most biological tissues in the red–near-infrared spectral region for modulation frequencies up to 1 GHz.

The linearity of Φ, $\ln(rU_{dc})$, and $\ln(rU_{ac})$ with respect to r have already been experimentally verified,[16] and the slope of the straight lines (let us call them S_Φ, S_{dc}, S_{ac}, respectively) can be measured with good precision, the uncertainty being of the order of a few percent. Furthermore, these slopes are sensitive with respect to μ_a and μ_s' as we can estimate from their derivatives with respect to μ_a and μ_s'. For typical values of ν (2.26×10^{10} cm/s), ω ($2\pi \times 60$ MHz), μ_a (0.05 cm^{-1}), and μ_s' (20 cm^{-1}), we have determined that S_Φ, S_{dc} and S_{ac} vary by ~5% as a consequence of a 10% variation in μ_a or in μ_s'. We analyzed the dependence of such a sensitivity on the modulation frequency, $\omega/2\pi$. The percentage variation of the slopes is essentially unaffected by ω, but their absolute variations show a different behavior. Although $\partial S_{dc}/\partial\mu$ (where μ indicates μ_a or μ_s') is obviously not dependent on ω and $\partial S_{ac}/\partial\mu$ is only slightly affected by the value of ω, $\partial S_\Phi/\partial\mu$ is more sensitive to changes in modulation frequency; its value is nearly doubled by the increase of $\omega/2\pi$ from 60 to 150 MHz. This dependence means that for higher modulation frequencies the phase slope is more sensitive to changes in μ_a and μ_s', but because the sensitivities of S_{dc} and S_{ac} are essentially the same, the overall sensitivity of the measurement is not drastically improved. The modulation frequency of 60 MHz, used in our experiment, can then be considered a good compromise between modulation efficiency and sensitivity to μ_a and μ_s' variations.

To determine the slopes in Eqs. (2)–(4) (S_Φ, S_{dc}, and S_{ac}), we collect data at different separation distances, which we call r_1 and r_2 with $r_1 < r_2$. If we define the quantities $\rho = r_2 - r_1$, $\varphi = \Phi(r_2) - \Phi(r_1)$, $\delta = \ln[r_2 U_{dc}(r_2)] - \ln[r_1 U_{dc}(r_1)]$, and $\alpha = \ln[r_2 U_{ac}(r_2)] - \ln[r_1 U_{ac}(r_1)]$, we can derive the following expressions:

$$\varphi = \rho\left(\frac{\nu^2\mu_a^2 + \omega^2}{\nu^2 D^2}\right)^{1/4} \sin\left[\frac{1}{2}\arctan\left(\frac{\omega}{\nu\mu_a}\right)\right], \quad (5)$$

$$\delta = -\rho\sqrt{\frac{\mu_a}{D}}, \quad (6)$$

$$\alpha = -\rho\left(\frac{\nu^2\mu_a^2 + \omega^2}{\nu^2 D^2}\right)^{1/4} \cos\left[\frac{1}{2}\arctan\left(\frac{\omega}{\nu\mu_a}\right)\right], \quad (7)$$

which are the phase factor, the intensity exponential factor, and the ac exponential factor, respectively, which display several useful characteristics.

(i) The quantities related to the excitation light source (A, S) have disappeared.

(ii) Experimentally measured quantities in spectroscopy are multiplied by an instrument response factor, which in general is a function of λ. Such a factor cancels in δ and α because they contain the ratio of U_{dc} and U_{ac} measured at different source–detector separations but at the same wavelength.

(iii) An analytical solution for μ_a, μ_s' and their errors can be obtained so that the data analysis is streamlined.

The determination of the analytical expressions for μ_a and μ_s' can be obtained in three different ways, because Eqs. (5)–(7) contain two unknowns ($\nu\mu_a$ and νD) and therefore are not independent. One can then choose to obtain μ_a and μ_s' from three different sets of measurements: φ and α, φ and δ, and δ and α. From a physical viewpoint this is due to the fact that φ, δ, and α have a different dependence on μ_a and μ_s'. The analytical expressions for the absorption coefficient and for the relative error in the three cases, obtained after some algebraic passages, are as follows. For δ, φ measurement (using dc and phase), we have

$$\mu_a = -\frac{\omega}{2\nu}\frac{\delta}{\varphi}\left(\frac{\varphi^2}{\delta^2} + 1\right)^{-1/2}, \quad (8)$$

$$\frac{\Delta\mu_a}{\mu_a} = \frac{2\varphi^2 + \delta^2}{\varphi^2 + \delta^2}\left[\frac{(\Delta\delta)^2}{\delta^2} + \frac{(\Delta\varphi)^2}{\varphi^2}\right]^{1/2}. \quad (9)$$

For α, φ measurement (using ac and phase), we have

$$\mu_a = \frac{\omega}{2\nu}\left(\frac{\varphi}{\alpha} - \frac{\alpha}{\varphi}\right), \quad (10)$$

$$\frac{\Delta\mu_a}{\mu_a} = \frac{\alpha^2 + \varphi^2}{\alpha^2 - \varphi^2}\left[\frac{(\Delta\varphi)^2}{\varphi^2} + \frac{(\Delta\alpha)^2}{\alpha^2}\right]^{1/2}. \quad (11)$$

For δ, α measurement (using dc and ac), we have

$$\mu_a = \frac{\omega}{2\nu}\frac{\delta}{\alpha}\left(\frac{\alpha^2}{\delta^2} - 1\right)^{-1/2}, \quad (12)$$

$$\frac{\Delta\mu_a}{\mu_a} = \frac{2\alpha^2 - \delta^2}{\alpha^2 - \delta^2}\left[\frac{(\Delta\delta)^2}{\delta^2} + \frac{(\Delta\alpha)^2}{\alpha^2}\right]^{1/2}. \quad (13)$$

The corresponding equations for the transport scattering coefficient and for its relative error are as follows.

For δ, φ measurement (using dc and phase) and δ, α measurement (using dc and ac), we have

$$\mu_s' = \frac{\delta^2}{3\mu_a\rho^2} - \mu_a, \quad (14)$$

$$\frac{\Delta\mu_s'}{\mu_s'} = 2\left[\frac{(\Delta\delta)^2}{\delta^2} + \frac{(\Delta\rho)^2}{\rho^2} + \left(\frac{\delta^2 + 3\mu_a^2\rho^2}{2\delta^2}\right)^2\frac{(\Delta\mu_a)^2}{\mu_a^2}\right]^{1/2}. \quad (15)$$

For α, φ measurement (using ac and phase), we have

$$\mu_s' = \frac{\alpha^2 - \varphi^2}{3\mu_a\rho^2} - \mu_a, \quad (16)$$

$$\frac{\Delta\mu_s'}{\mu_s'} = 2\left\{\frac{\alpha^2(\Delta\alpha)^2 + \varphi^2(\Delta\varphi)^2}{(\alpha^2 - \varphi^2)^2} + \frac{(\Delta\rho)^2}{\rho^2} + \left[\frac{\alpha^2 - \varphi^2 + 3\mu_a^2\rho^2}{2(\alpha^2 - \varphi^2)}\right]^2\frac{(\Delta\mu_a)^2}{\mu_a^2}\right\}^{1/2}. \quad (17)$$

The choice of the coupled quantities among α, δ, and φ from which we determine μ_a is based on the evaluation of the uncertainties $\Delta\mu_a/\mu_a$, which also affect the uncertainties $\Delta\mu_s'/\mu_s'$ as shown by Eqs. (15) and (17). In our measurement, $\Delta\alpha/\alpha$, $\Delta\delta/\delta$, and $\Delta\varphi/\varphi$ were of the same order of magnitude (a few percent), so we chose the measurement scheme that has the smallest factor multiplying the quantity of the square roots in Eqs. (9); (11); and (13). Under our experimental conditions these factors are approximately 1 for the (α, φ) and (δ, φ) measurement (because $\varphi \ll \alpha, \delta$), whereas in the ($\alpha$, δ) measurement the multiplying factor is almost an order of magnitude larger, 8–10 (because $\alpha \approx \delta$). Furthermore, the fact that the error on dc quantities is somewhat smaller than that on ac quantities, and the fact that the dc signal is higher than the ac signal, prompted us to choose the (δ, φ) scheme and Eqs. (8) and (9) for obtaining μ_a and its relative error. The use of dc and phase in frequency-domain measurements was also suggested as an alternative to a phase and modulation measurement.[15] We observe that from Eqs. (6) and (7) it can be shown that $|\alpha| > |\delta|$ holds as a general result, i.e., the ac component of light attenuates more than the dc component. In fact, the ac attenuation is larger at higher modulation frequencies, whereas the dc attenuation is independent of ω.

In principle, one could also apply the scheme of a double measurement to a two-frequency method, but

this approach would not yield a superior result because the measured quantities are less sensitive to changes in ω than to changes in r. This contention is shown quantitatively by the fact that, for practical values of Δr and $\Delta\omega$ (let us say $\Delta r \sim 2$ cm and $\Delta\omega \sim 2\pi \times 100$ MHz), and neglecting the dependence of A and S on ω, we obtain

$$\frac{\partial \Phi}{\partial r}\,\Delta r \geq \int_{\omega-\Delta\omega}^{\omega} \frac{\partial \Phi}{\partial \omega'}\,d\omega'. \tag{18}$$

$$\left|\frac{\partial \ln(rU_{ac})}{\partial r}\right| \Delta r \gg \int_{\omega-\Delta\omega}^{\omega} \left|\frac{\partial \ln(rU_{ac})}{\partial \omega'}\right| d\omega'. \tag{19}$$

The ratios between the two sides of inequalities (18) and (19) are shown in Figs. 3(a) and 3(b) for different values of μ_a as a function of $\omega/2\pi$. Actually, in general, the modulation (A) and the dc component (S) of the excitation light source do depend on ω. This dependence implies that in a two-frequency measurement the quantities related to the excitation light source do not disappear. Introducing $\alpha_\omega = \ln[rU_{ac}(\omega_2)] - \ln[rU_{ac}(\omega_1)]$, from Eq. (4) we obtain

$$\alpha_\omega = -r\sqrt{\frac{\mu_a}{2D}}\left(\left\{\left[1+\left(\frac{\omega_2}{\nu\mu_a}\right)^2\right]^{1/2}\right\}^{1/2} - \left\{1+\left[1+\left(\frac{\omega_1}{\nu\mu_a}\right)^2\right]^{1/2}\right\}^{1/2}\right) + \ln\left[\frac{S(\omega_2)A(\omega_2)}{S(\omega_1)A(\omega_1)}\right],$$

and the last term must be taken into account. Here S and A are unknown and a general procedure for a two-frequency measurement should somehow eliminate them, e.g., if we reference α_ω to a direct measurement of the dc and ac components of the source. Of course, this procedure is affected by an error and it cannot be successfully accomplished if the term containing S and A is much greater than the one containing μ_a and μ_s'. Such was the case for the LED we used; in our case, the two-frequency scheme turned out to be inapplicable. The preceding discussion based on inequalities (18) and (19) is general because the independence of S and A on ω is the best condition for a two-frequency measurement.

We based our measurements of μ_a and μ_s' on a two-distance technique. In practice we collect the data at two source–detector distances (r_1, r_2) and calculate φ and δ. From Eqs. (8) and (14) we then obtain the values of the absorption and scattering coefficients. From Eqs. (9) and (15) we calculate the relative errors in these quantities. This procedure, applied wavelength by wavelength within the whole spectral region covered by the LED (620–700 nm), allows us to get the spectra of μ_a and μ_s'. Recalling that in our protocol $r_1 < r_2$, we choose the two source–detector separations r_1 and r_2 on the following basis: the difference $r_2 - r_1$ is required to be as large as possible because the precision of the measurement is improved for large values of $r_2 - r_1$. The constraints on the value of $r_2 - r_1$ arise from the fact that

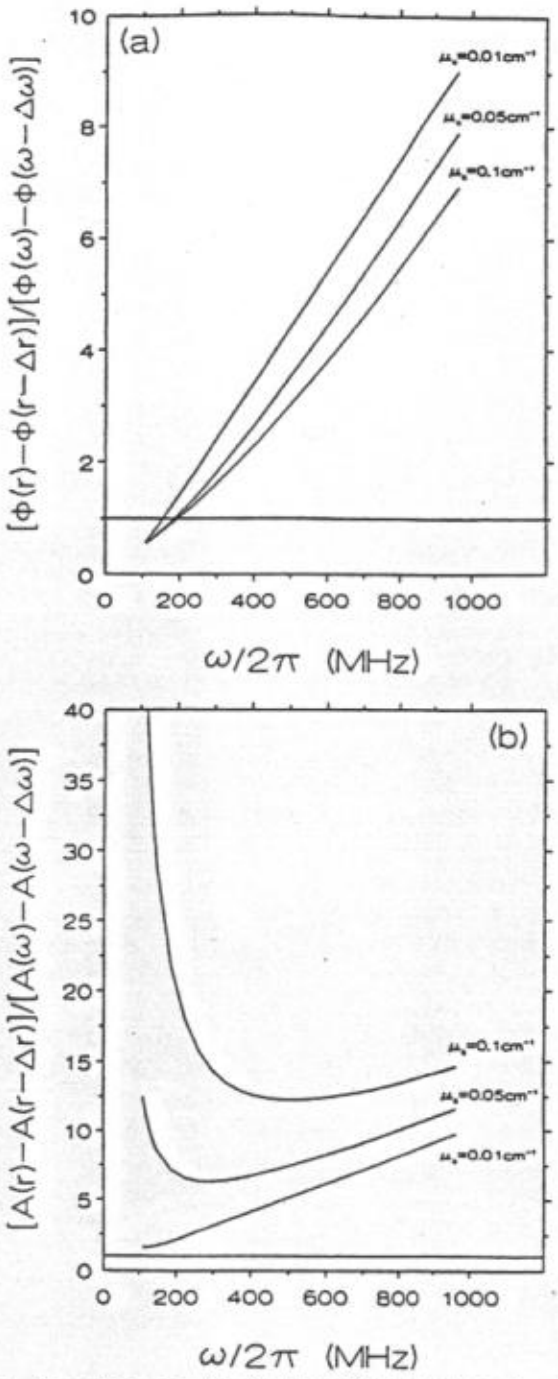

Fig. 3. Dependence on $\omega/2\pi$ for three different values of μ_a of (a) $[\Phi(r,\omega) - \Phi(r-\Delta r,\omega)]/[\Phi(r,\omega) - \Phi(r,\omega-\Delta\omega)]$, (b) $[\ln(rU_{ac})|_{r,\omega} - \ln(rU_{ac})|_{r-\Delta r,\omega}]/[\ln(rU_{ac})|_{r,\omega} - \ln(rU_{ac})|_{r,\omega-\Delta\omega}]$, where $r = 4$ cm, $\Delta r = 2$ cm, $\Delta\omega/2\pi = 100$ MHz. We indicate $\ln(rU_{ac})$ with A on the y axis of (b). We note that the quantities on the y axis in (a) and (b) are the ratio of the right-hand to the left-hand sides of inequalities (18) and (19), respectively. The horizontal line in each plot corresponds to the equivalence of the variations of Φ and $\ln(rU_{ac})$ relative to changes in r and ω. The two-distance technique is more sensitive than the two-frequency method in the region where the curves are above the horizontal line.

r_1 must be much greater than the photon mean-free path [in order for Eqs. (5)–(7) to be valid], and r_2 must allow for the detection of an adequate light signal (both dc and ac intensities decay exponentially with

distance). We choose r_1 to be 1.5 cm, whereas r_2 varies from 4.0 to 2.5 cm, depending on the amount of absorber in the medium.

3. Results

First we measured the absorption and scattering coefficient spectra of the Liposyn solution containing no MB absorber (a blank). The results are shown in Fig. 4, in which μ_a is essentially the absorption coefficient of water and μ_s' is the scattering coefficient caused by the particles suspended in the solution. The former is in good agreement with both the order of magnitude of water absorbance and with its known spectral dependence.[19] We subtract this spectrum of μ_a from the spectrum of the MB solution to obtain the corrected absorption spectra for MB alone. The measured value of μ_s' at 630 nm ($20.2 \pm 1.2\ cm^{-1}$) is close to the value predicted by van Staveren *et al.*[20] for the transport scattering coefficient of 1.54% Intralipid at 632.8 nm ($20.6\ cm^{-1}$). Even if they considered a different scattering material, this agreement suggests that the value we measured is of the correct order of magnitude. Furthermore, the spectral dependence of μ_s' that they calculated by using Mie theory is similar to the one we measured. They found $d\mu_s'/d\lambda = -0.03\ cm^{-1}/nm$ at 660 nm, which is comparable with our value of $-0.040 \pm 0.006\ cm^{-1}/nm$.

The quantitative absorption spectra of MB dissolved in the Liposyn solution are measured for concentrations up to 0.450 μM in increments of 0.045 μM. The spectra obtained are shown in Figs. 5(a) and 5(b), whereas in Fig. 6 the spectra measured for MB concentrations of 0.090, 0.225, and 0.450 μM are compared with those obtained with the spectrophotometer for the same concentrations of MB diluted in water instead of in a strongly scattering medium. The good quantitative agreement is evident. We studied the behavior of μ_a and μ_s' as a function of absorber concentration at various wavelengths. We found that μ_s' is unaffected by MB concentrations at all the wavelengths we considered [the results at 620, 640, 660, 680, and 700 nm are shown in Fig. 7(a)].

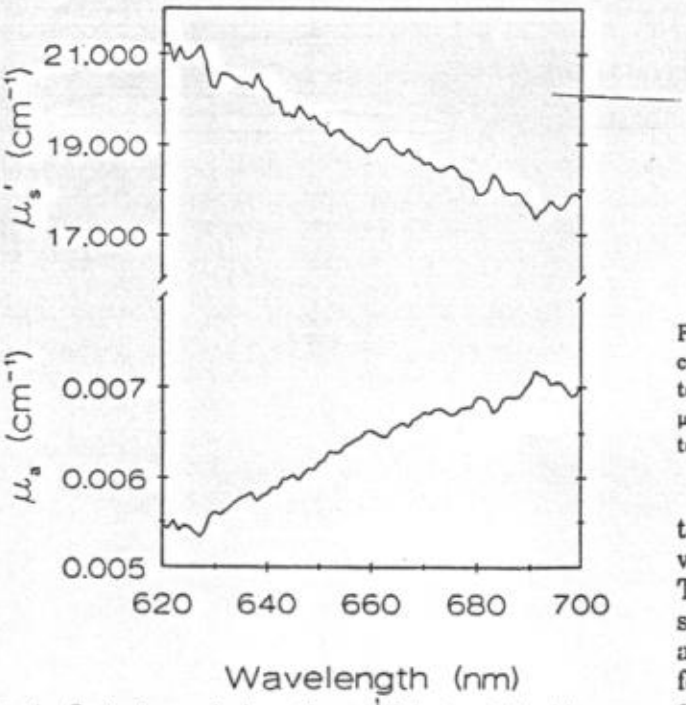

Fig. 4. Scattering and absorption coefficients of the Liposyn solution containing no MB.

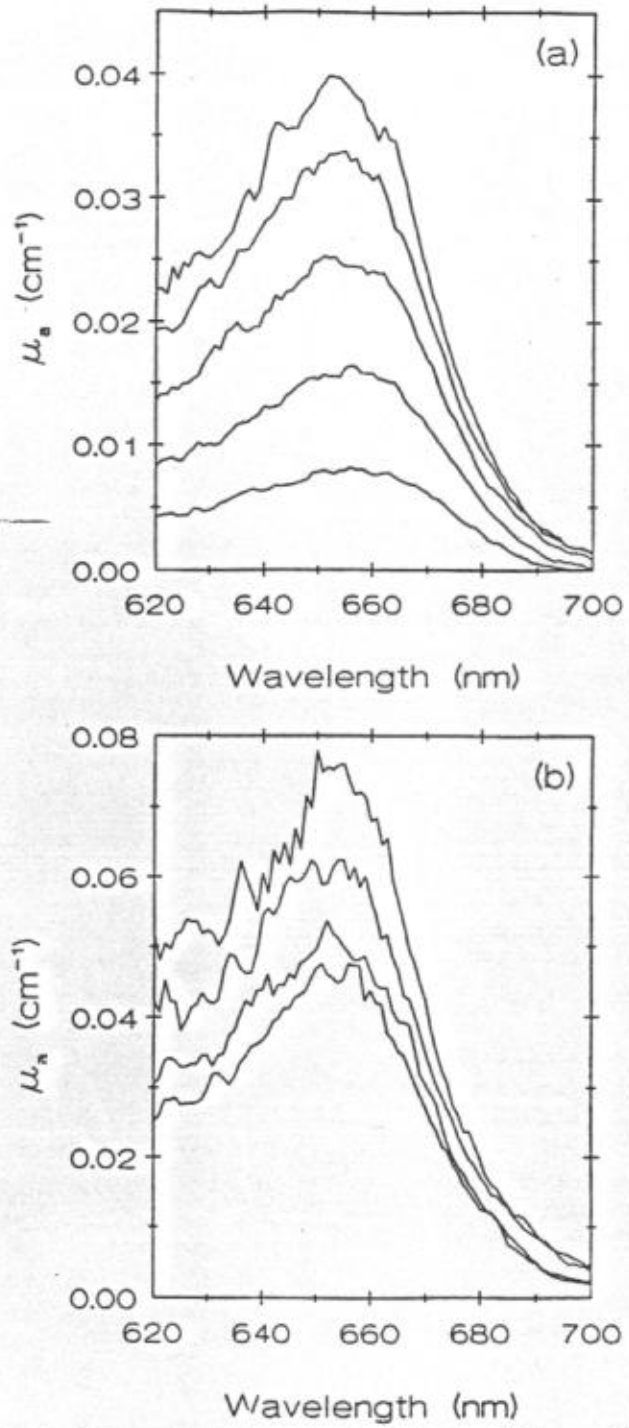

Fig. 5. Spectra of MB absorption coefficients at different MB concentrations in the Liposyn solution. The various spectra refer to MB concentrations of (a) 0.045, 0.090, 0.135, 0.180, and 0.225 μM; (b) 0.270, 0.315, 0.360, and 0.450 μM. The spectrum relative to 0.405 μM is not shown for clarity.

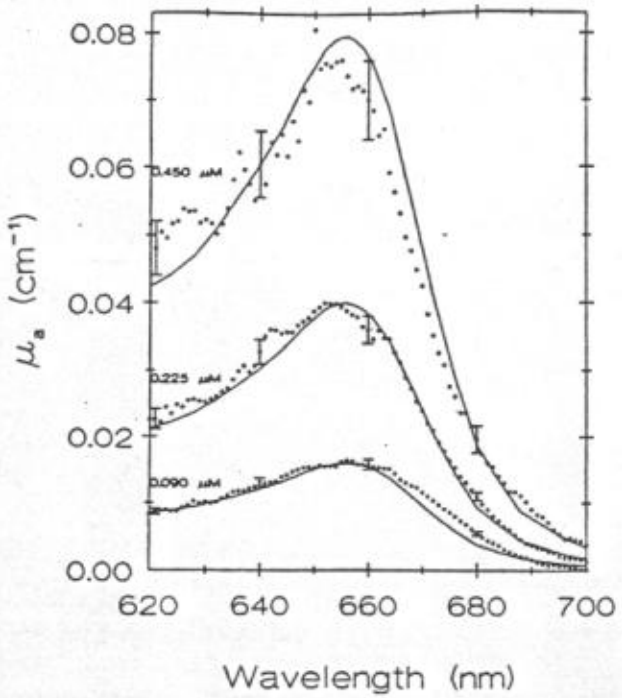

Fig. 6. Quantitative comparison between MB absorption coefficient spectra measured in the strongly scattering medium by the LED technique (filled circles) and in a nonscattering regime by a spectrophotometer (curves). The spectra correspond to MB concentrations of 0.090, 0.225, and 0.450 μM as labeled. Errors bars for the experimental data relative to the strongly scattering medium are shown every 20 nm.

In contrast, μ_a shows a linear dependence on MB concentration as predicted by the Beer–Lambert law, Eq. (1), and as we also expected in a multiple scattering regime. The experimental points and the best straight lines among them are shown in Fig. 7(b) for the absorption coefficient values measured at 620, 640, 660, 680, and 700 nm. These results, $\partial\mu_s'/\partial[c] = 0$ and $\partial\mu_a/\partial[c] = K(\lambda)$, where K is a function only of λ, are in agreement with what Patterson *et al.*[15] found in a similar experiment at a single wavelength.

4. Discussion

The quantitative measurement of absorption spectra in strongly scattering media is of great interest in biomedical applications. Studies of this kind have been conducted on rat liver[10] and on a number of substances (potatoes, bovine muscle and liver, calf brain, and various aqueous suspensions containing absorbers such as MB and Photofrin II)[21] with an integrated transmittance and reflectance measurement technique. However, one cannot apply this technique to *in vivo* measurements. A method that has been applied *in vivo* is time-dependent reflectance spectroscopy, which led researchers to the quantitative determination of μ_a at several wavelengths for the normal tissue of a cat in which phthalocyanine photosensitizer was injected.[22] The disadvantages of this technique are its inability to monitor dynamic processes in real time and the complexity of the instrumentation.

The LED method we describe here is promising both from a general viewpoint (the possibility of having a white efficiently modulated light source in the region from 600 to 900 nm with excellent stability

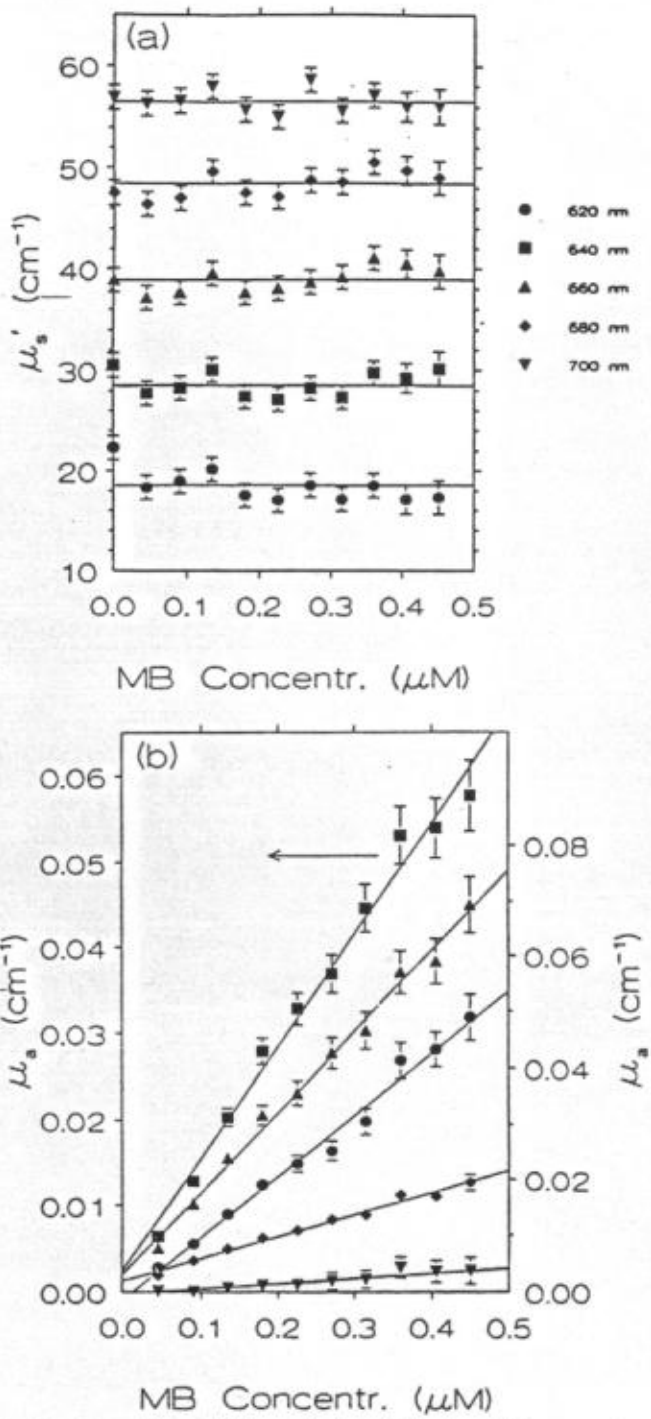

Fig. 7. Dependence of the optical coefficients on MB concentration at five wavelengths. (a) scattering coefficient (a progressive offset of 10, 20, 30, and 40 cm^{-1} has been added to the points relative to 640, 660, 680, and 700 nm, respectively); (b) absorption coefficient (the left scale refers only to the points relative to 640 nm). Straight lines were obtained by a weighted least-squares method. When the error bars are not displayed they are of the order of the symbol dimensions.

characteristics) and from a practical viewpoint (the relatively low cost, light and compact instrumentation, and the safe and almost straightforward application to *in vivo* spectroscopy of biological tissues). In addition, the fast acquisition times of the frequency-domain measurement, which can be as short as 10 ms, permit one to monitor changes dynamically in optical properties of tissues that, for *in vivo* measurements, can be related to metabolic processes.

The calculations and experimental protocol presented here are based on an infinite medium geometry, and hence they are not directly applicable to noninvasive *in vivo* optical spectroscopy. The method for obtaining spectra *in vivo* is, however, almost identical to the measurement technique described in Subsection 2.D. The only difference is that for *in vivo* measurements the LED and the tip of the detector optical fiber are held against the surface of the medium rather than being immersed in the medium, and hence it is convenient for us to assume that the geometry of the tissue sample under investigation *in vivo* is a uniform semi-infinite medium. This may be a reasonable assumption if the tissue volume under investigation is relatively uniform with dimensions much larger than the source–detector separation. One may employ a method of images, described by Patterson *et al.*,[14] to obtain frequency-domain expressions from the diffusion approximation for the phase shift Φ, U_{dc}, and U_{ac} of the signal detected at the surface of the medium. By assuming that the source–detector separation r is much greater than the photon mean-free path, one may manipulate the calculated quantities of Φ, U_{dc}, and U_{ac} for the semi-infinite geometry to yield expressions containing μ_a and μ_s', which are formally identical to the expression of Eqs. (5)–(7). This allows for the use of Eqs. (8)–(17) for the determination of μ_a and μ_s' by the use of the two-distance method described in this paper. We are currently testing the validity of the expressions for a semi-infinite medium.

It is relevant that the two-distance method gives a better determination of the scattering and absorption coefficients than the use of two modulation frequencies. Of course, if multiple modulation frequencies can be employed, then multiple determination of the quantity Φ can provide us enough information to determine both μ_a and μ_s'. However, as shown by Svaasand *et al.*,[23] a relatively wide frequency range must be employed.

In conclusion, to the best of our knowledge this research represents the first quantitative spectral determination of the absorption and scattering coefficients of a chromophore in a highly scattering medium through the use of a LED as a light source.

The experimental research and the analysis of the data were performed at the Laboratory for Fluorescence Dynamics in the Department of Physics at the University of Illinois at Urbana–Champaign. This laboratory is supported jointly by the Division of Research Resource of the National Institutes of Health (RR03155) and the University of Illinois at Urbana–Champaign; this research was supported by grant CA 57032. We thank W. W. Mantulin for the useful discussions and the critical reading of the manuscript.

References and Notes

1. G. Wagnieres, C. Depeursinge, P. Monnier, M. Savary, P. Cornaz, A. Chatelain, and H. van den Bergh, "Photodetection of early cancer by laser induced fluorescence of a tumor-selective dye: apparatus design and realization," in *Photodynamic Therapy: Mechanisms II*, T. J. Dougherty, ed., Proc. Soc. Photo-Opt. Instrum. Eng. **1203**, 43–52 (1990).
2. M. S. Patterson, B. C. Wilson, J. W. Feather, D. M. Burns, and W. Pushka, "The measurement of dihematopotphyrin ether concentration in tissue by reflectance spectrophotometry," Photochem. Photobiol. **46**, 337–343 (1987).
3. M. Cope and D. T. Delpy, "System for long-term measurement of cerebral blood and tissue oxygenation on newborn infants by near infrared transillumination," Med. Biol. Eng. Comput. **26**, 289–294 (1988).
4. B. C. Wilson and M. S. Patterson, "The physics of photodynamic therapy," Phys. Med. Biol. **31**, 327–360 (1986).
5. S. L. Jacques and S. A. Prahl, "Modeling optical and thermal distribution in tissue during laser irradiation," Laser Surg. Med. **6**, 494–503 (1987).
6. W. F. Cheong, S. A. Prahl, and A. J. Welch, "A review of the optical properties of biological tissues," IEEE J. Quantum Electron. **26**, 2166–2185 (1990).
7. F. F. Jöbsis, J. H. Keizer, J. C. LaManna, and M. Rosenthal, "Reflectance spectrophotometry of cytochrome aa_3 *in vivo*," J. Appl. Physiol. **43**, 858–872 (1977).
8. E. Gratton, "Method for the automatic correction of scattering in absorption spectra by using the integrating sphere," Biopolymers **10**, 2629–2634 (1971).
9. R. R. Anderson and J. A. Parrish, "Optical properties of human skin," in *The Science of Photomedicine*, J. D. Regan and J. A. Parrish, eds. (Plenum, New York, 1982).
10. P. Parsa, S. L. Jacques, and N. S. Nishioka, "Optical properties of rat liver between 350 and 2200 nm," Appl. Opt. **28**, 2325–2330 (1989).
11. T. J. Farrel, M. S. Patterson, and B. Wilson, "A diffusion theory model of spatially resolved, steady-state diffuse reflectance for the noninvasive determination of tissue optical properties *in vivo*," Med. Phys. **19**, 879–888 (1992).
12. K. M. Yoo, Y. Takiguchi, and R. R. Alfano, "Dynamic effect of weak localization on the light scattering from random media using ultrafast laser technology," Appl. Opt. **28**, 2343–2349 (1989).
13. R. Araki and I. Nashimoto, "Near-infrared imaging *in vivo*: imaging of Hb oxygenation in living tissues," in *Time-Resolved Spectroscopy and Imaging of Tissues*, B. Chance and A. Katzir, eds., Proc. Soc. Photo-Opt. Instrum. Eng. **1431**, 321–322 (1991).
14. M. S. Patterson, B. Chance, and B. C. Wilson, "Time resolved reflectance and transmittance for the noninvasive measurement of tissue optical properties," Appl. Opt. **28**, 2331–2336 (1989).
15. M. S. Patterson, J. D. Moulton, B. C. Wilson, K. W. Berndt, and J. R. Lakowicz, "Frequency-domain reflectance for the determination of the scattering and absorption properties of tissue," Appl. Opt. **30**, 4474–4476 (1991).
16. J. B. Fishkin and E. Gratton, "Propagation of photon-density waves in strongly scattering media containing an absorbing semi-infinite plane bounded by a straight edge," J. Opt. Soc. Am. A **10**, 127–140 (1993).

17. Aldrich Chemical Company Laboratories, Milwaukee, Wisconsin, 1993.
18. B. A. Feddersen, D. W. Piston, and E. Gratton, "Digital parallel acquisition in frequency domain fluorometry," Rev. Sci. Instrum. **60**, 2929–2936 (1989).
19. N. E. Dorsey, ed., *Properties of Ordinary Water-Substance*, (Reinhold, New York, 1940).
20. H. J. van Staveren, C. J. M. Moes, J. van Marie, S. A. Prahl, and M. J. C. van Gemert, "Light scattering in Intralipid-10% in the wavelength range of 400–1100 nm," Appl. Opt. **30**, 4507–4514 (1991).
21. J. L. Karagiannes, Z. Zhang, B. Grossweiner, and L. I. Grossweiner, "Applications of the 1-D diffusion approximation to the optics of tissues and tissue phantoms," Appl. Opt. **28**, 2311–2317 (1989).
22. M. S. Patterson, J. D. Moulton, B. C. Wilson, and B. Chance, "Applications of time-resolved light scattering measurements to photodynamic therapy dosimetry," in *Photodynamic Therapy: Mechanisms II*, T. J. Dougherty, ed., Proc. Soc. Photo-Opt. Instrum. Eng. **1203**, 62–75 (1990).
23. L. O. Svaasand, B. J. Tromberg, R. C. Haskell, T.-T. Tsay, and M. W. Berns, "Tissue characterization and imaging using photon density waves," Opt. Eng. **32**, 258–266 (1993).